Sandwich-Type Ferromagnetic RF Integrated Inductor

Masahiro Yamaguchi, Makoto Baba, and Ken-Ichi Arai

***Abstract*—The first demonstration of a sandwich-type ferromagnetic RF integrated spiral inductor for the 2-GHz range is reported. Two ferromagnetic CoNbZr films were set to sandwich the spiral in order to enhance the amount of magnetic flux linkage across the coil current. The stresses given from the insulator to the ferromagnetic film were studied. The inductance L of 7.9 nH and the qualify factor Q of 12.7 were obtained for a 200 μm $\times$ 400 μm size four-turn rectangular spiral at $f = 2$ GHz. The inductance was better than that of an air core of the same coil size by 19%, and the Q was better by 23%. Comparison with the on-top magnetic film type was also discussed.**

***Index Terms*—Inductors, integrated circuit fabrication, magnetic films, magnetic resonance, magnetic susceptibility.**

I. Introduction

THERE IS A strong demand for high-quality integrated passives for RF circuitry. The primary interest for the integrated inductors is to obtain a high quality factor Q, which is in most cases achieved by the reduction of losses and parasitic capacitances. The method of loss reduction was to utilize thick and low-resistivity metal to reduce coil resistance [1], [2], as well as to employ high-resistivity semiconductor substrate or to form a cavity beneath the coil to reduce eddy currents in the substrate [3]. Stacked coil was also tried in order to save the coil area and to increase the mutual inductance but the coil resistance was doubled. Thus, it is not easy to achieve a high-Q factor and the size reduction simultaneously.

A new approach to solve this problem is to apply ferromagnetic thin films to the RF integrated inductor. The original idea is to enhance the magnetic flux associated with the coil current and accordingly to enhance the inductance and quality factor of the inductor. A ferromagnetic RF integrated inductor with performance higher than an air core spiral has been pioneered by the authors and its use is spreading to other research groups [4].

Our first trial was the on-top type ferromagnetic inductor for the 1-GHz range. We simply applied a ferromagnetic film on top of an integrated spiral [5], [6]. The performance obtained for a four-turn square spiral of a 377 $\times$ 377 μm^2 area CoNbZr soft ferromagnetic film with AlSi coil material was $L = 7.6$ nH, $R = 6.8\,\Omega$, and $Q = 7.1$ at 1 GHz. This work has demonstrated that the ferromagnetic film enhanced the inductance without any degradation of the quality factor in the 1-GHz range. The rate of the inductance enhancement, however, was only 12% of the conventional air-core spiral of the same size.

Manuscript received March 21, 2001; revised August 26, 2001. This work was supported in part by the Japan Society of Promotion of Science under the Grant-in-Aid for Scientific Research 12305025 and under the Grant-in-Aid for Scientific Research Priority Areas (A), "Highly Functionized Global Interface Integration," 13025202.

M. Yamaguchi and K.-I. Arai are with the Research Institute of Electrical Communication, Tohoku University, Sendai 980-8577, Japan (e-mail: yamaguti@riec.tohoku.ac.jp).

M. Baba was with the Research Institute of Electrical Communication, Tohoku University, Sendai 980-8577, Japan. He is now with the Mitsubishi Electric Corporation, Amagasaki, Japan.

Publisher Item Identifier S 0018-9480(01)10461-8.

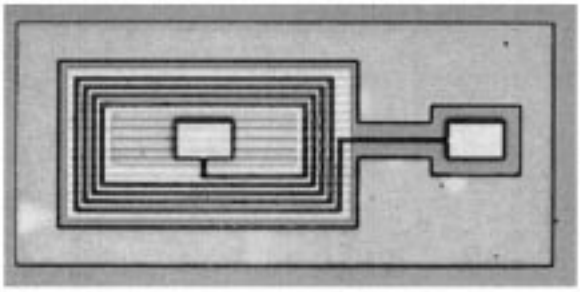

Fig. 1. Outlook of the fabricated sandwich-type ferromagnetic RF integrated inductor (200 $\times$ 400 μm^2).

In this paper, a new sandwich-type ferromagnetic RF integrated inductor for a 2-GHz application was microfabricated. The two ferromagnetic CoNbZr films sandwich the spiral to enhance the magnetic flux linkage across the coil current. The performance obtained was $L = 7.9$ nH and $Q = 12.7$ at 2 GHz for a 200 $\times$ 400 μm^2 size four-turn rectangular spiral.

II. Structure and Design

Currently, the magnetic films usable for the RF inductor are available only by sputter-deposition. Each film has uniaxial anisotropy with the easy axis of magnetization oriented along a certain direction in the film plane. In the RF range, the permeability along the hard axis of magnetization is much higher than the permeability along the easy axis of magnetization, which is at a right angle to the hard axis. This is because the rotational magnetization process governs the magnetic flux reversal along the hard axis, while the magnetic domain movement and resulting large eddy current losses are significant along the easy axis. Therefore, hard axis excitation effectively increases the amount of magnetic flux associated with the coil current and accordingly the inductance of the inductor.

The rectangular coil shape employed in this work is preferable for such a uniaxial magnetic film because the magnetic film area for the hard axis excitation is larger than that of a square spiral and a round spiral.

Fig. 1 shows the outlook of the fabricated a 200 $\times$ 400 μm^2 spiral inductor. Two ferromagnetic $Co_{85}Nb_{12}Zr_3$ (atomic percent) amorphous films sandwich the spiral with an SiO_2 in-

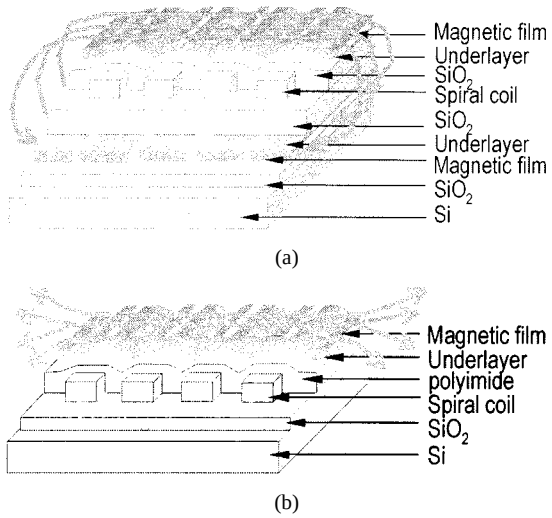

Fig. 2. Two types of ferromagnetic RF integrated inductors. (a) Sandwich type. (b) On-top type.

sulator in between. The CoNbZr film is a known soft magnetic material with zero magnetostriction at the composition of $Co_{85}Nb_{12}Zr_3$. The direction and the intensity of the magnetic easy axis orientation of the CoNbZr film is controllable by the magnetic field annealing with good production reproducibility. The hard axis of magnetization is in the vertical direction in the figure. Magnetic field from the coil current is applied to the hard axis direction at the top and bottom legs of the spiral, which contributes to enhance the amount of magnetic flux. On the other hand, the magnetic field at the left and right legs of the spiral is applied along the easy axis direction. Here, the amount of magnetic flux remains unchanged.

In detail, the magnetic films are applied to narrow slits along the length of the spiral, as shown in Fig. 2(a). These slits or the magnetic wire array structure increase the demagnetizing field along the flux path. Therefore, the effective magnetic anisotropy field H^k increases. This greatly helps to enhance the ferromagnetic resonance (FMR) frequency of the magnetic film and to make a broad-bandwidth inductor [7].

As compared with the on-top type inductor shown in Fig. 2(b), the sandwich-type inductor has the following advantages.

1) The amount of magnetic flux linkage across the coil current is larger. Therefore, the inductance and the quality factor are enhanced.
2) The amount of magnetic flux leakage is smaller. Therefore, electromagnetic interference (EMI) to the integrated circuits and devices should be insignificant.
3) Eddy current losses in substrate should be smaller because of low-level leakage flux.

In the cross-sectional view of Fig. 3, t_c is the coil thickness, w_c the coil width, d_c the coil spacing, t_m the magnetic film thickness, w_m the slitted magnetic wire width, and d_m the magnetic film wire spacing. The dimensions of fabricated inductors are listed in the left-most column in Table I. Each coil has four turns with 3-μm thickness, 8-μm width, and 3-μm spacing. The thickness of the magnetic film wire is also a constant of

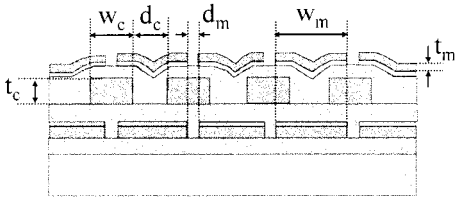

Fig. 3. Cross-sectional view of the sandwich-type inductor.

0.1 μm. The permeability and FMR frequency are a function of the width, spacing, and thickness of the wires. As mentioned for Fig. 2, this technique is useful to adjust apparent magnetic properties to the desired operation frequency range. The on-top type inductors are listed in Table I for comparison. Note that the on-top type inductors are almost twice as large (377×377 μm^2) as the sandwich-type one and have a square spiral coil.

III. Insulator

Magnetic permeability is usually sensitive to stress because of magnetostriction. In Fig. 2(a), the bottom magnetic layer is stressed by the stacked over-layers, especially by the insulator deposited next to the bottom magnetic layer. The degree of stress depends on the material of the insulator. Therefore, two kinds of 4-μm-thick dielectric materials were compared. A photosensitive polyimide film (Toray, UR3100 series) is easily processed and patterned to the thickness of a few micrometers. It is known, however, that its volume shrinks by 50% after curing, which might result in large amount of stress. The other candidate was a sputter-deposited SiO_2 film with careful stress control by the sputtering gas pressure.

In the experiments, three wafers were commonly processed as follows. An 0.1-μm-thick amorphous $Co_{85}Nb_{12}Zr_3$ soft magnetic film and a 5-nm-thick Ti film were RF-sputter deposited in turn on a soda glass substrate in a vacuum chamber. The Ti layer is to have a good adhesion between the magnetic film and the insulator. The CoNbZr–Ti double layer is then applied through ion milling to get a 4-mm-long 8-μm-wide micro wire array structure with 3-μm spacing. The 363 parallel wires were patterned to occupy 4×4 mm^2 area in total. This size is so designed to have good signal-to-noise ratio (SNR) during magnetic measurements. The slits were made along the easy axis of magnetization. Slitting a single large film provides the benefit of reducing internal stress of the magnetic film. This structure and its dimensions will be used in the real fabrication of the inductor in this work.

This is the completion of a reference test sample wafer that has no overcoat. The second wafer was then spun-coat with photosensitive polyimide film and cured at a temperature of no higher than 360 °C. The cured polyimide film was 4-μm thick. The third wafer was RF-sputter deposited onto the 4-μm-thick SiO_2 film with an Ar gas pressure of 2.8×10^{-4} torr, an O_2 gas pressure of 1.2×10^{-4} torr, and an electric power of 200 W. A 3-in-diameter SiO_2 target was used. The deposition rate was 0.71 μm/h.

Magnetization curves were measured by a vibrating sample magnetometer (VSM). In Fig. 4, the reference CoNbZr mag-

TABLE I
SPECIFICATIONS AND CHARACTERISTICS OF THE FABRICATED FERROMAGNETIC RF INTEGRATED INDUCTORS

	1GHz			2GHz		
(Unit: μm)	L(nH)	R(Ω)	Q	L(nH)	R(Ω)	Q
Sandwich type						
air(w_c=8,d_c=3,t_c=3)(Cu)	6.23	5.09	7.81	6.67	8.16	10.3
no slit	9.14(+47%)	13.08	4.46(-43%)	6.14(-7.9%)	46.96	1.65(-84%)
w_m=9,d_m=2,t_m=0.1	6.86(+10%)	5.73	7.64(-2.2%)	8.06(+21%)	10.56	9.62(-6.7%)
w_m=8,d_m=3,t_m=0.1	6.68(+7.2%)	5.43	7.85(+0.5%)	7.83(+17%)	7.82	12.61(22%)
w_m=7,d_m=4,t_m=0.1	6.75(+8.3%)	5.09	8.46(+8.3%)	**7.94(+19%)**	**7.86**	**12.72(+23%)**
On-top type						
air(w_c=11,d_c=11,t_c=2.7)(Al-Si)	6.66	6.85	6.15	7.35	15.72	5.91
w_m=10.25,d_m=0.75,t_m=0.1	**7.38(+11%)**	**7.51**	**6.27(+2.0%)**	8.62(+17%)	20.81	5.22(-12%)
w_m=9.5,d_m=1.5,t_m=0.1	7.34(+10%)	7.6	6.16(+0.1%)	**8.25(+12%)**	**18.54**	**5.57(-5.8%)**

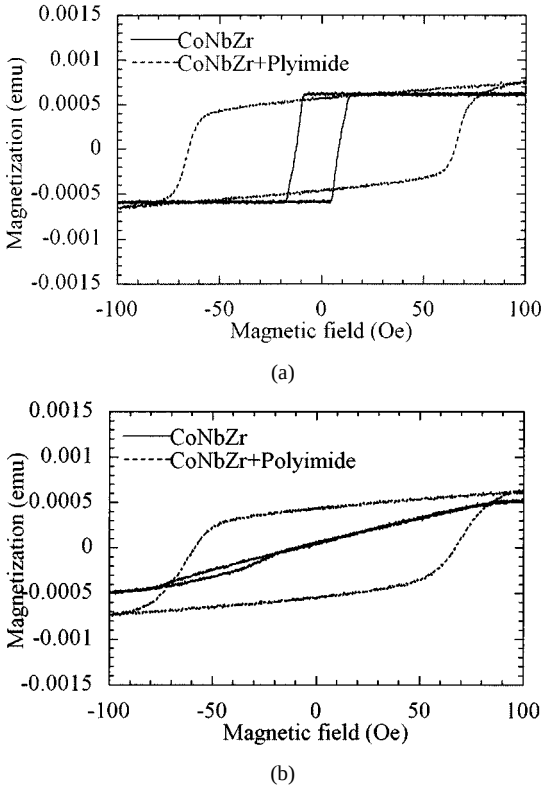

Fig. 4. Magnetization curve of an 0.1-μm-thick CoNbZr film covered with a 4-μm-thick polyimide film. (a) Along the easy axis direction. (b) Along the hard axis direction.

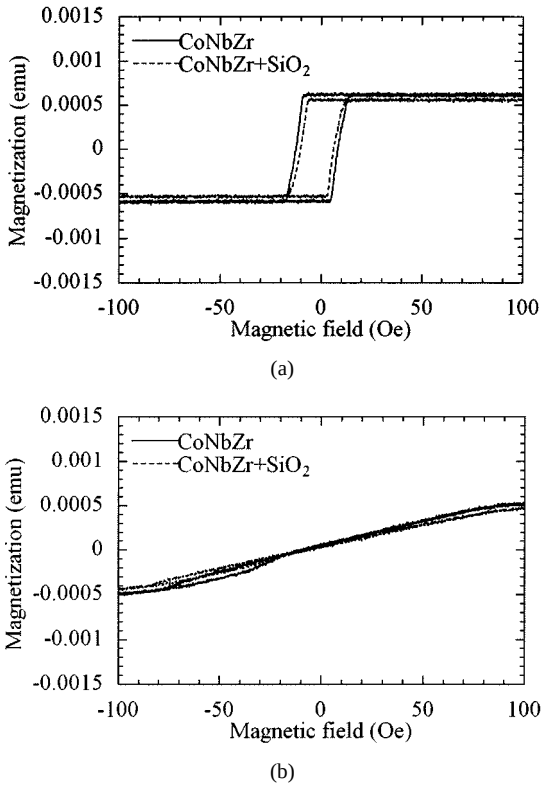

Fig. 5. Magnetization curve of an 0.1-μm-thick CoNbZr film covered with a 4-μm-thick SiO_2 film. (a) Along the easy axis direction. (b) Along the hard axis direction.

netic film without the overcoat exhibited good anisotropic characteristics, showing a square hysteresis loop along the easy axis and a flat loop along the hard axis. The coercive force along the easy axis was well below 10 Oe and that along the hard axis was negligible. With a polyimide overcoat, however, the coercive force of both the easy and the hard axis directions degraded to 60 Oe and the film was no longer anisotropic because of the strong stress from the cured polyimide film. On the other hand, the SiO_2 overcoat did not damage the magnetic characteristics if the SiO_2 film was deposited under the written gas pressure and electric power, as shown in Fig. 5. Therefore, the SiO_2 overcoat was used to the inductor fabrication.

In detail, the magnetization curve of the reference sample did not close as shown in the bottom left of Figs. 4(b) and 5(b). This is because of the residual magnetization of the electromagnet used in our VSM (Tamagawa Works Co).

IV. FABRICATION PROCESS

As shown in Fig. 6, a 1.4-μm-thick SiO_2 layer was formed on a (100)-oriented n-type Si wafer with resistivity of 500 Ωcm or higher by wet thermal oxidization and LPCVD. The 0.1-μm-thick CoNbZr film was then RF-sputter deposited and then ion-milled to form the bottom magnetic wire array structure. Followed by the RF-sputter deposition of a 3-μm-thick SiO_2 insulator, a 3-μm-thick Cu film was RF-sputter deposited and liftoff to form the four-turn rectangular spiral. The top SiO_2 and CoNbZr ferromagnetic layers were then formed just the same

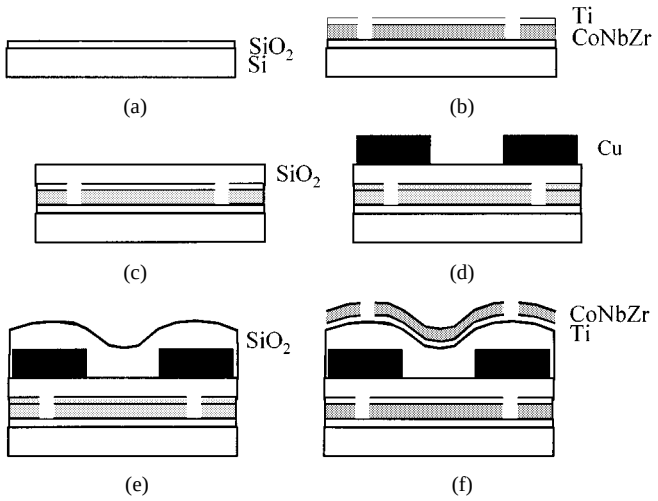

Fig. 6. Fabrication process. (a) SiO_2 deposition by wet oxidization and LPCVD. (b) Bottom CoNbZr/Ti RF-sputter deposition and micro patterning by ion milling. (c) Bottom SiO_2 deposition by RF sputtering and patterning by liftoff. (d) Cu RF-sputter deposition and patterning by liftoff. (e) Top SiO_2 deposition by RF sputtering and patterning by liftoff. (f) Top Ti/CoNbZr RF-sputter deposition and micro patterning by ion milling.

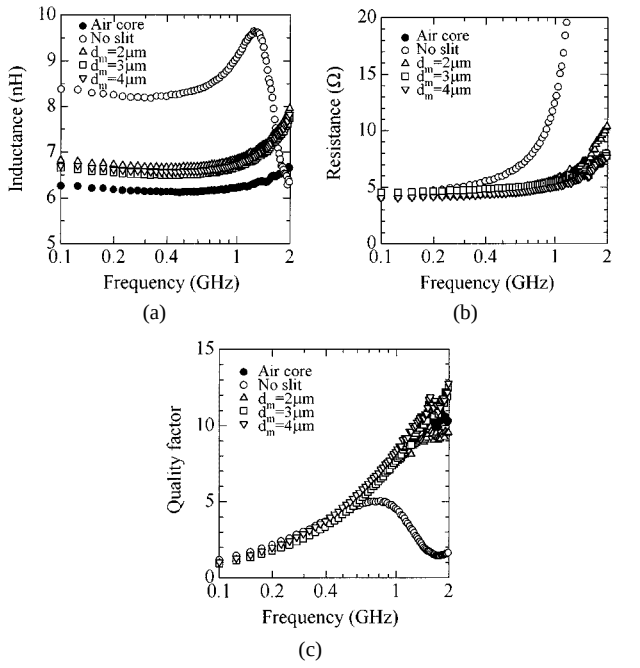

Fig. 7. Measured electric characteristics. (a) Inductance. (b) Resistance. (c) Quality factor.

as were the bottom layers. The top and bottom magnetic layers were applied the 5-nm-thick Ti underlayer films.

These processes can be completed as the post-Si processes. This is a great feature to integrate ferromagnetic inductors.

V. High-Frequency Characteristics

Fig. 7 shows the measured high-frequency characteristics of the sandwich inductors. A wafer probe (GGB Industries, Picoprobe Model-10) and a network analyzer (HP 8720D) were used to extract the impedance parameters. Major results at 1 GHz and 2 GHz are summarized in Table I. The reference air core exhibited $L = 6.8$ nH and $Q = 10.3$ at 2 GHz.

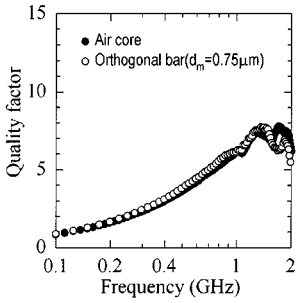

Fig. 8. Quality factor of the on-top type ferromagnetic RF integrated inductor.

In Fig. 7(a), the inductance of each ferromagnetic inductor was higher than the air core inductance. In the low frequency range, the inductor with no-slit ferromagnetic film showed the highest inductance, achieving $L = 9.1$ nH at 1 GHz. The value obtained was higher than the air core's by 47%. This is because of high permeability of the no-slit ferromagnetic film. With raising the drive frequency, however, the inductance degraded because of the low FMR frequency of the no-slit ferromagnetic film. The influence of the FMR is also seen as the increase of resistance in Fig. 7(b) and the degradation of the quality factor in Fig. 7(c).

The ferromagnetic inductors with micro wire array film structure exhibited as high quality factor as the air core up to 2 GHz. The best performance was $L = 7.9$ nH and $Q = 12.7$ at 2 GHz obtained for the ferromagnetic wire width of 7 μm and its spacing of 4 μm. The inductance was higher by 19% and the quality factor was better by 23% than the air core.

In the case of the on-top type inductors, quality factor was maxim between 1 GHz and 2 GHz, and the value obtained was less than 8 as shown in Fig. 8. Thus the quality factor and the bandwidth of the sandwich type inductor are advantageous to those of the on-top type inductor. This is because: 1) design of slit work was optimized for the 2-GHz band; 2) the amount of magnetic flux per unit area was larger; and 3) stray capacitance might be smaller.

Further improvement should be possible by optimizing the magnetic film thickness with optimum slit work, terminating the top and bottom magnetic layers at their edges, and employing a magnetic film with higher anisotropy field and higher saturation magnetization.

VI. Conclusion

First microfabrication of a sandwich-type ferromagnetic RF integrated spiral inductor over a 2-GHz range is demonstrated. The two ferromagnetic CoNbZr films sandwich the spiral to enhance the magnetic flux linkage across the coil current. An inductance of 7.9 nH and a qualify factor of 12.7 were obtained for a 200 μm $\times$ 400 μm four-turn rectangular spiral at $f = 2$ GHz. The inductance was better than that of an air core of the same coil size by 19%, and the quality factor was better by 23%.

Acknowledgment

The authors wish to acknowledge Dr. S. Tanabe and Dr. K. Itoh, Mitsubishi Electric Company, for helpful discussions. The

authors are also grateful to Prof. Y. Nakamura and Prof. H. Muraoka of RIEC, EAC of RIEC, the Laboratory for Electronic Intelligent Systems of RIEC, and Venture Business Laboratory, each in Tohoku University for microfabrication facilities.

REFERENCES

[1] V. Ilderem, S. Bigelow, R. Braithwaite, F. Chai, P. Dahl, V. DelaTorre, S. Hildreth, C. Jasper, J. John, M. Kaneshiro, T. Keller, C. Kyono, I.-S. Lim, C. Moorer, K. Moore, C. Ramiah, J. Steele, J. Teplik, S. Wipf, Y. Yang, H. Zhao, and D. Zupac, "RF BiCMOS process technologies at Motorola," in *IEEE Radio Frequency Integrated Circuits Symp. Workshop Notes*, June 2000.

[2] M. Gouker, K. Konistis, J. Knecht, L. Kushner, and L. Travis, "Multi-layer spiral inductors in a high-precision fully-planar MCM-D process," in *IEEE MTT-S Int. Microwave Symp. Dig.*, vol. 2, June 2000, pp. 1055–1058.

[3] H. Jiang, Y. Wang, J.-L. A. Yeh, and N. C. Tien, "Fabrication of high-performance on-chip suspended spiral inductors by micromachining and electroless copper plating," in *IEEE MTT-S Int. Microwave Symp. Dig.*, vol. 1, June 2000, pp. 279–283.

[4] D. S. Gardnar, A. M. Crawford, and S. Wang, "High frequency (GHz) and low resistance integrated inductors using magnetic materials," in *Int. Interconnect Technol. Conf.*, June 2001, pp. 101–103.

[5] M. Yamaguchi, K. Suezawa, K. I. Arai, Y. Takahashi, S. Kikuchi, W. D. Li, Y. Shimada, S. Tanabe, and K. Ito, "Microfabrication and characteristics of magnetic thin-film inductors for 1 GHz-drive mobile communication handset applications," *J. Appl. Phys.*, vol. 85, pp. 7919–7922, Apr. 1999.

[6] M. Yamaguchi, M. Baba, K. Suezawa, T. Moizumi, K. I. Arai, Y. Shimada, A. Haga, S. Tanabe, and K. Itoh, "Magnetic RF integrated thin-film inductors," in *IEEE MTT-S Int. Microwave Symp. Dig.*, vol. 1, June 2000, pp. 205–208.

[7] M. Yamaguchi, K. Suezazwa, M. Baba, K. I. Arai, Y. Shimada, S. Tanabe, and K. Itoh, "Application of bi-directional thin-film micro wire array to RF integrated spiral inductors," *IEEE Trans. Magn.*, vol. 36, pp. 3514–3517, Nov. 2000.

Masahiro Yamaguchi was born on October 7, 1956. He received the B.S., M.S., and Dr.Eng. degrees from Tohoku University, Sendai, Japan, in 1979, 1981, and 1984, respectively.

He is currently an Associate Professor at the Research Institute of Electrical Communication (RIEC), Tohoku University. His research interests are integrated micromagnetic devices, related high-frequency measurements, and electromagnetic compatibility (EMC).

Dr. Yamaguchi is the chairman of the Special Committee on Micromagnetic Devices of the Institution of Electrical Engineers of Japan.

Makoto Baba was born on July 22, 1976. He received the B.S. and M.S. degrees from Tohoku University, Sendai, Japan, in 1991 and 2001, respectively.

While at Tohoku University, he investigated the ferromagnetic RF integrated inductors. He is currently with the Mitsubishi Electric Corporation, Amagasaki, Japan.

Ken-Ichi Arai was born on February 23, 1943. He received the B.S. and Dr.Eng. degrees from Tohoku University, Sendai, Japan, in 1966 and 1971, respectively.

He is currently a Professor at the Research Institute of Electrical Communication (RIEC), Tohoku University. His research interests include electromagnetic materials and bio-magnetic sensor-actuator systems.

Prof. Arai is a member of the Science Council of Japan.